Optimizing the Friction Welding Parameters to Maximize Tensile Strength of SUS 304HCu Austenitic Stainless Steel Tube Joints

M. Vinoth Kumar, Research Scholar; **V. Balasubramanian,** Professor

Centre for Materials Joining & Research (CEMAJOR), Department of Manufacturing Engineering,
Annamalai University, Annamalai Nagar- 608 002, Tamil Nadu, India.

ABSTRACT

The SUS 304HCu austenitic stainless steel is used in superheater / reheater of ultra super critical boilers for their high temperature oxidation and corrosion resistance. Cu addition to steels can have adverse effects on the mechanical properties during fusion welding as it can form low temperature eutectic phases that preferentially segregate to the grain boundaries and embrittle the alloy. Friction welding is a solid state welding process where the bonding takes place well below the melting temperature of the alloy, combined with the autogenous nature of this welding process minimizes the adverse effects of low temperature eutectics segregation. Hence, in this investigation an attempt has been made to develop an empirical relationship to predict the tensile strength of the friction welded SUS 304HCu tubes of 57.1 mm outer diameter and 3.5 mm thick using statistical tools such as design of experiments, analysis of variance and regression analysis. Response surface methodology was used to optimize the process variables and maximum joint efficiency of 99% was achieved using the optimized friction welding variables.

Keywords : SUS 304HCu; Friction welding; Design of experiments; Tensile properties.

1.0 INTRODUCTION

The SUS 304HCu austenitic steel is used in the finishing stages of superheater / reheater tubing for super critical boilers for their high temperature oxidation and corrosion resistance. The addition of 3 wt. % Cu to SUS 304HCu, aimed at increasing the corrosion resistance has found to increase the elevated temperature strength, especially their creep performance in the temperature range of 650°-750° C. The addition of Cu to steels can have adverse effects on the mechanical properties during fusion welding as it can form low temperature eutectic phases that preferentially segregate to the grain boundaries and embrittle the alloy [1]. Friction welding is a solid state welding process where the bonding takes place well below the melting temperature of the alloy combined with the autogenous nature of this welding process minimizes the adverse effects of low temperature eutectics segregation.

Koen et al [2] developed a new variant of friction welding process for joining of pipelines. The process is a 'one shot' completely automatic process which can produce quality welds independent of the operator's skill and can offer advantages on environmental issues. This indicates the need for establishing a welding procedure for joining of pipes / tubes by friction welding. Kimura et al [3] successfully friction welded the AISI 310S austenitic stainless steel pipe of thickness 1.5 mm with 100% joint efficiency and studied the effect of welding parameters which concludes that minimum friction pressure with forging pressure double as that of friction pressure is required to attain a fully efficient joint, also reported that the minimum thickness of the pipe that can be friction welded is 0.5mm. Yuanzhi et al [4] investigated the strength distribution across the inertia friction welded dissimilar joint of Inconel 751 and Austenite Steel 21-4N which is highly heat and corrosion resistant. The friction welded joint between the Inconel 751 and Austenite Steel 21-4N has been used in working temperatures ranging from 600° C to 800° C. This indicates that friction welding can be successfully applied for welding of austenitic stainless steel joints for high temperature application.

Mumin [5] investigated the microstructure and hardness variation at the interfaces of friction welded AISI 304 austenitic stainless steel joint. It was reported that continuous drive friction welding can be successfully used for fabrication of austenitic stainless steel by proper selection of optimum welding parameters and statistical analysis can be used as an economical and reliable tool in optimizing the friction welding parameters. Satyanarayana et al [6] studied the microstructure and mechanical properties of the friction welded austenitic–ferritic stainless steel dissimilar joint along with the optimization of the friction welding parameters. Sathiya et al [7] optimized the friction welding process parameter for welding of similar joints of AISI 430 ferritic stainless steel that produces maximum tensile strength and minimum metal loss. The metal loss tends to increase with increasing friction time and the optimized input values friction joints exhibited higher quality.

From the literature review it is understood that friction welding is commonly used for making joints with rods and the literature is scarce as far as the friction welding of tubes or pipes. In particular, friction welding of SUS 304HCu stainless steel tubes has not been reported so far. Hence, in this investigation an attempt has been made to develop an empirical relationship to optimize the friction welding parameters and predict the tensile strength of the friction welded SUS 304HCu austenitic stainless steel tube joint using statistical tools such as design of experiments, analysis of variance and regression analysis.

2 EXPERIMENTAL WORK

2.1 Parent material properties

The parent materials used in the investigation were tubes of 57.1 mm outer diameter and 3.5 mm thick SUS 304HCu austenitic stainless steel. The chemical composition of the parent material is given in **Table 1** and the mechanical properties of the parent material are given in **Table 2**.

Table 1 : Chemical composition (wt %) of the parent material SUS 304HCu tube

C	Si	Mn	P	S	Cr
0.086	0.23	0.81	0.021	0.0003	18.18
Ni	**N**	**Cu**	**Nb**	**B**	**Al**
9.06	0.095	3.080	0.045	0.0039	0.01

2.2 Finding the working limits of the welding parameters

In order to find the feasible working limit of the friction welding parameters for welding the SUS 304HCu tubes. The most influencing parameters in friction welding were identified from the literature as (i) Rotational speed, (ii) Friction pressure, (iii) Friction time, (iv) Forging pressure, and (v) Forging time. Owing to the machine and fixture limitations on the load that can be applied during the welding of jobs of this size and configuration, the friction pressure and forging pressure were kept constant.

Table 2 : Tensile properties of the parent material SUS 304HCu tube

0.2% Yield strength in MPa	Tensile strength in MPa	% Elongation in gauge length of 50 mm
308	613	43.2

From the literature [5-9] it is known that, friction and forging pressure are directly related to geometry and material properties of parts to be welded. The forging pressure has to be kept higher than that of the friction pressure to achieve good joint and hence, the forging pressure was selected to be 90% (47 MPa) of the machines forging capacity. The friction pressure to be selected such that enough friction is created to generate sufficient heat required to plasticize the material. The friction pressure was selected to 60% (32 MPa) of the machine's capacity. A series of systematic trails has been conducted to determine the feasible working limit of each parameter to be varied during this study. The macrographs of the joints fabricated outside the feasible working limits are shown in the **Fig. 1**. The working limit was fixed based on the defect free macrostructure and minimum metal loss.

(i) The **Fig. 1a** shows the macrograph of the joint welded at rotational speed < 1200 RPM which was not bonded due to insufficient heat generation by friction.

(ii) The **Fig. 1b** shows the macrograph of the joint welded at rotational speed > 2400 RPM which reveals defect formation in the joint due to the excess heat generation.

(iii) The **Fig. 1c** shows the macrograph of the joint welded at friction time < 20 s which reveals less flash formation due to the insufficient friction time.

(iv) The **Fig. 1d** shows the macrograph of the joint welded at friction time > 40 s which reveals excess flash formation due to the higher friction time.

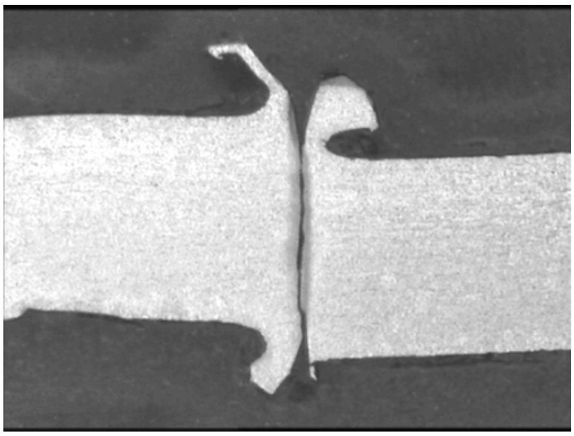

a. Rotational Speed (R) < 1200 RPM

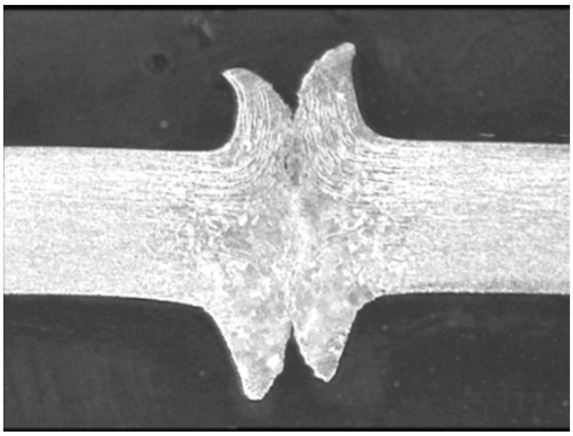

b. Rotational Speed (R) > 2400 RPM

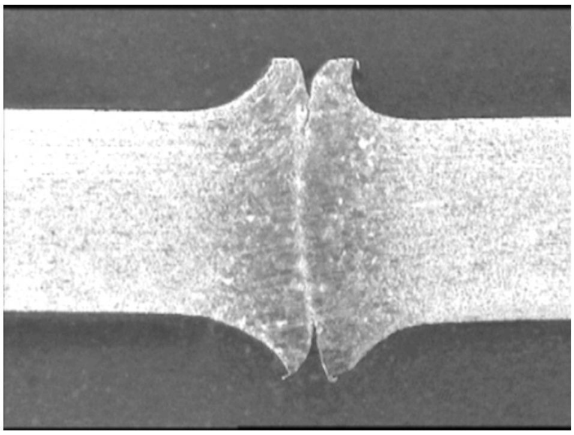

c. Friction time < 20 s

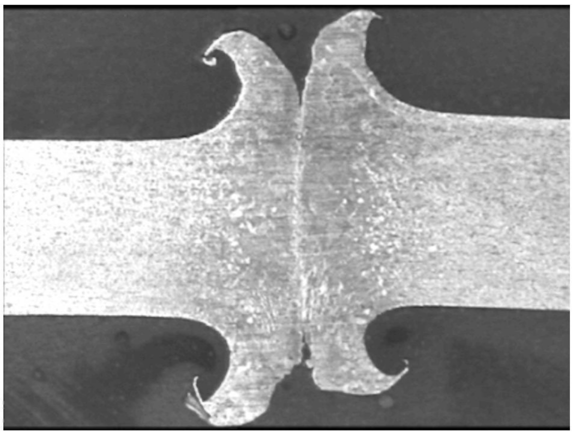

d. Friction time > 40 s

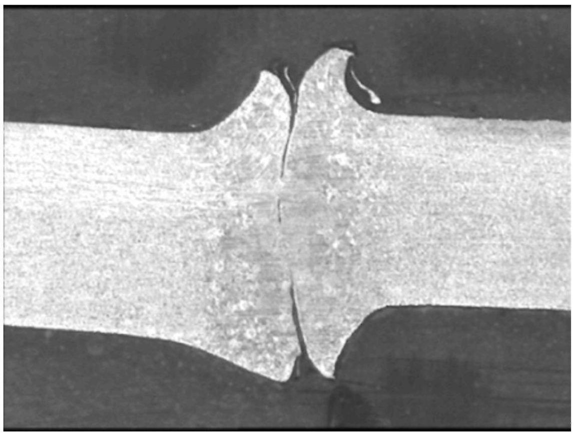

e. Forging time < 30 s

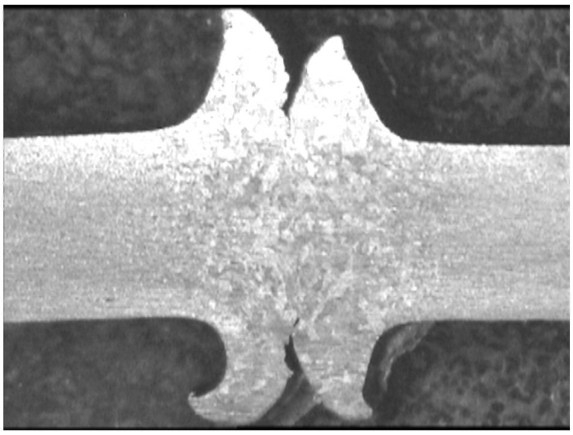

f. Forging time > 60 s

Fig. 1 : Macrograph of the joint fabricated outside the feasible working limits (at 5X Mag.)

(v) **The Fig. 1e** shows the macrograph of the joint welded at forging time < 30 s which reveals lack of bonding at the interface due to lesser forging time.

(vi) The **Fig. 1f** shows the macrograph of the joint welded at forging time > 60 s which reveals excess flashing on one side of the joint due to higher forging time.

2.3 Developing experimental matrix and fabrication of joints

A 3 factor and 5 level central composite rotatable design matrix (small) consisting of 15 trials was selected to prescribe the experimental (welding) conditions. The chosen welding parameters and the level at which they were varied based on the feasibility limit was shown in **Table 3.** The experimental design matrix consisting of 15 sets of coded condition and comprising a full replication 3 factor factorial design of 4 points, 6 star points, and 5 center points shown in the **Table 4** was used. The method of designing such a matrix was dealt elsewhere [10].

All the variables at 0 level are the center points, while the combination of a particular variable at the lowest (-1.41) or the highest level (+1.41) with the other variables at intermediate (0) level are known as the star points. The coded value for the intermediate levels can be calculated from the following relationship.

$$X_i = 1.41\ [2X - (X_{max} + X_{min})] / (X_{max} - X_{min}) \quad (1)$$

Where,

X_i is the required coded value of a variable X;

X_{min} is the lowest level of the variable;

X_{max} is the highest level of the variable;

X is any value of the variable from X_{min} to X_{max};

Table 3 : Feasible working range of friction welding parameters

S. No	Parameter	Notation	Unit	Levels				
				-1.41	-1.0	0	+1.0	+1.41
1	Rotational Speed	R	RPM	1200	1376	1800	2224	2400
2	Friction time	F	s	20	23	30	37	40
3	Forging time	D	s	30	34	45	56	60

Table 4 : Design matrix and experimental results

Expt. No.	R	F	D	R (RPM)	F (s)	D (s)	Tensile strength of the joint (MPa)
1	1	1	-1	2224	37	34	591
2	1	-1	1	2224	23	56	599
3	-1	1	1	1376	37	56	374
4	-1	-1	-1	1376	23	34	358
5	-1.41	0	0	1200	30	45	316
6	1.41	0	0	2400	30	45	573
7	0	-1.41	0	1800	20	45	534
8	0	1.41	0	1800	40	45	526
9	0	0	-1.41	1800	30	30	536
10	0	0	1.41	1800	30	60	542
11	0	0	0	1800	30	45	553
12	0	0	0	1800	30	45	551
13	0	0	0	1800	30	45	555
14	0	0	0	1800	30	45	553
15	0	0	0	1800	30	45	552

The friction welded joint of SUS 304HCu tubes is shown in the **Fig. 2a**. The tensile specimens were extracted by wire cut electric discharge machining, transverse to the weld joint as shown in the **Fig. 2b**. The schematic representation and the photograph of the tensile specimen are shown in the **Fig. 2c** and **Fig. 2d** respectively. The tensile tests were carried out in accordance with the ASTM E 8M-04 standard in a 100 kN, electro-mechanical controlled universal testing machine.

a. Photograph of friction welded tube joint

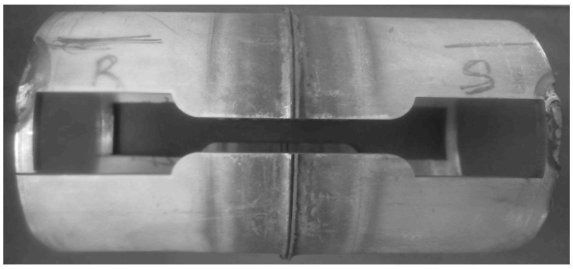

b. Scheme of specimen extraction

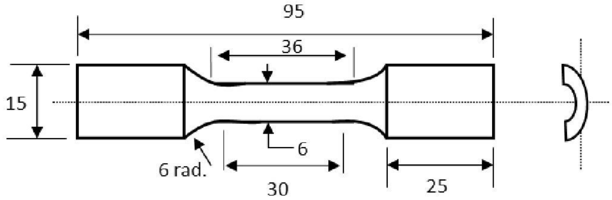

c. Schematic representation of tensile specimen

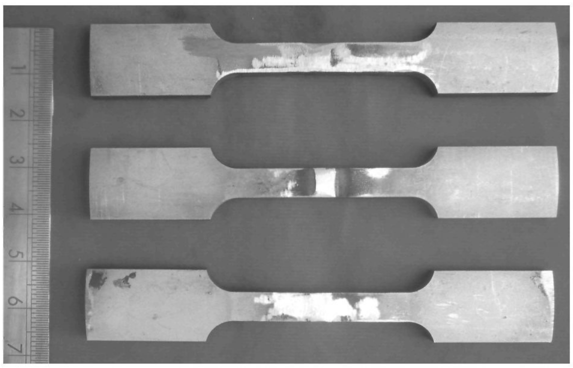

d. Tensile specimen photograph

Fig. 2 : Details of the friction welded joint and tensile specimen

3.0 DEVELOPING EMPIRICAL RELATIONSHIP

The response, tensile strength of the friction welded joints can be expressed as a function of the friction welding parameters such as rotational speed (R), friction time (F), and forging time (D).

$$\text{Tensile strength} = f\{R,F,D\} \tag{2}$$

The second order polynomial (regression) equation is used to represent the response surface of Y (Tensile strength) is given by [10-12].

$$Y = b_o+\sum b_i x_i+\sum b_{ii} x_i^2+\sum b_{ij} x_i x_j+\varepsilon, \tag{3}$$

and for three factors, the selected polynomial could be expressed as

$$Y(\text{Tensile Strength}) = \{b_o+b_1(R)+b_2(F)+b_3(D)+b_{12}(RF)+b_{13}(FD)+b_{23}(DR)+b_{11}(R^2)+b_{22}(F^2)+b_{33}(D^2)\} \tag{4}$$

Where, bo is the average of responses and b_1, b_2, b_3,..., b_{44} are regression coefficients that depend on respective linear, interaction, and squared term of factors. The value of the coefficient was calculated using Design Expert software. The significance of the each coefficient was determined by Fisher's test and the results are presented in **Table 5**. The final empirical relationship was constructed using only significant coefficients and the developed empirical relationship is given below:

Tensile strength of the joint =

$$\{-1696.50+1.38(R)+29.32(F)+16.72(D)-0.0013(RF)-0.00103(RD)-0.308(FD)-0.0003(R^2)-0.226(F^2)-0.0604(D^2)\}\ \text{MPa} \tag{5}$$

The adequacy of the developed model tested using the analysis of variance (ANOVA) technique and the results of second order response model fitting in the form of ANOVA is given in **Table 5**. As per this technique, if the value Prob > F is < 0.05 then the model terms are significant. By applying the same criteria for the model terms also, it is known that all the model terms are significant. The lack of fit is not significant as desired. The coefficient of determination (R^2) indicates the goodness of the fit for the model. In this case, the value of determination coefficient (R^2=0.99) indicates that the only < 1% of the total variation was not explained by the model.

The value of adjusted determination coefficient (Adj R^2=0.99) is also high, which indicates a high significance of the model. Predicted R^2 is also in a good agreement with the adjusted R^2. Adequate precision compares the range of predicted values at

Table 5: ANOVA test results for tensile strength model

Source	Sum of squares (SS)	Degrees of freedom (DOF)	Mean square (MS)	F-Value	P-value Prob > F	*Whether significant or not?
Model	109113.3966	9	12123.71074	6732.86302	< 0.0001	Significant
R-Rotational Speed	33024.5	1	33024.5	18340.04783	< 0.0001	Significant
F-Friction Time	32	1	32	17.77109512	0.0084	Significant
D-Forging Time	18	1	18	9.996241003	0.0250	Significant
RF	27.82869379	1	27.82869379	15.45457388	0.0111	Significant
RD	46.54545455	1	46.54545455	25.84886562	0.0038	Significant
FD	1123.447123	1	1123.447123	623.9026773	< 0.0001	Significant
R^2	22539.51246	1	22539.51246	12517.24437	< 0.0001	Significant
F^2	976.9625886	1	976.9625886	542.5529715	< 0.0001	Significant
D^2	370.9918349	1	370.9918349	206.0290995	< 0.0001	Significant
Residual	9.00338437	5	1.800676874			
Lack of Fit	0.20338437	1	0.20338437	0.092447441	0.7762	Not Significant
Std. Dev.	1.3418930188107		R-Squared		0.999917493	
Mean	514.2		Adj R-Squared		0.99976898	
C.V. %	0.260967137		Pred R-Squared		0.999675236	
PRESS	35.4390382		Adeq Precision		258.0471848	
* Values of p value "Prob > F" less than 0.0500 indicate the model terms are significant.						

the design points to the average prediction error. A relatively lower value of the coefficient of variation (C.V.%=0.26) indicates improved precision and reliability of the conducted experiments [12-15].

Fig. 3 shows the high correlation existing between the experimental values and the predicted values as the residual are fallen in a straight line (**Fig. 3a**), which means the errors are normally distributed. In **Fig. 3b** the predicted value from the model is compared with the observed value and found to have a good fit with each other.

4.0 OPTIMIZATION

The optimization module in Design Expert statistical software package based on response surface methodology (RSM) was used as an optimization tool to search the optimum values of the process variables. The optimization was done by choosing the desired goal as maximizing the tensile strength. The response graphs generated by the software were shown in **Fig. 4.**

The 3D response graphs were developed by taking two parameters in the 'X' and 'Y' axes and the response in 'Z' axis. The apex point in the response surface graph represents the optimal point and this optimum condition to achieve maximum tensile strength was predicted with reasonable precision. The predicted optimum parameters to achieve maximum tensile strength of the friction welded SUS 304HCu austenitic stainless steel was given in **Table 6.**

The **Fig. 4** shows the perturbation plot showing the effects of all the welding parameters on the tensile strength of the friction welded joint. The perturbation plot shows that the tensile strength initially increases linearly with the increase in

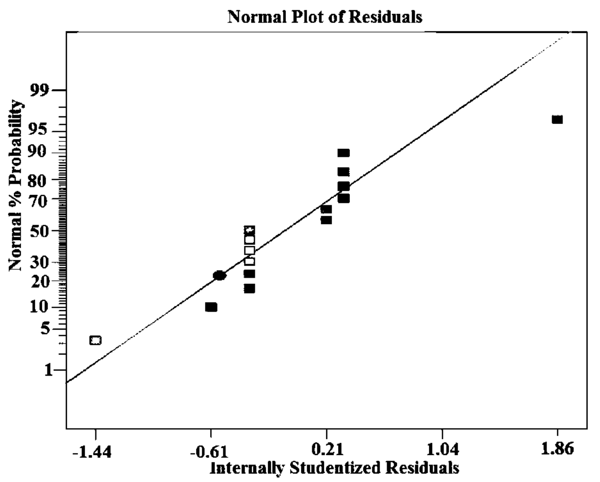

a. Normal probability plot of residuals

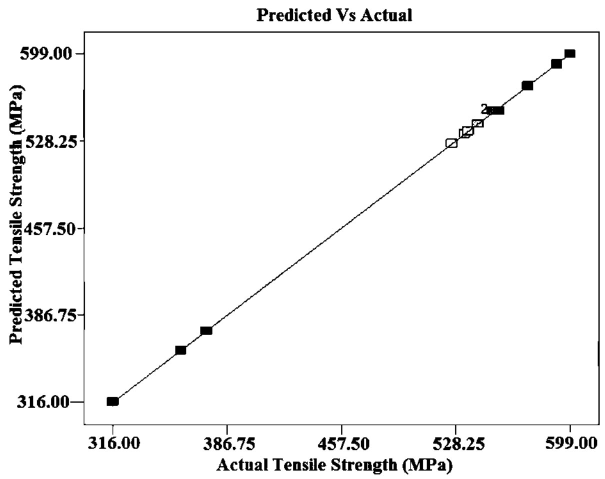

b. Plot of predicted Vs actual

Fig. 3 : Correlation graph

rotational speed and the slopes down after reaching the maximum value. The rotational speed has the maximum effect on the response when compared with rest of the parameters. The **Fig. 5a** shows the 3D surface response plot showing the effect of rotational speed (R) and Friction time (F) on tensile strength at D = 55.1 s. The maximum tensile strength is obtained at the peak of the apex where the friction pressure is 23.73 s and the forging time is 55.1 s. The **Fig 5b** shows the 3D surface response plot showing the effect of rotational speed (R) and forging time (D) on tensile strength at F = 23.73 s.

The maximum tensile strength is obtained at the peak of the apex where the rotational speed (R) 2112.23 RPM and the forging time (D) is 55.1 s. The **Fig. 5c** shows the 3D surface response plot showing the effect of friction time (F) and forging time (D) on tensile strength at rotational speed (R) = 2112.23 RPM. The maximum tensile strength is obtained at the peak of the apex where the friction time (F) is 23.73 s and the forging time (D) is 55.1 s. The transverse tensile properties of the friction welded joint of SUS 304HCu austenitic stainless steel fabricated using optimized parameters was given in **Table 7**. The predicted tensile strength for the optimized parameter is 607 MPa whereas the experimentally attained tensile strength is 599 MPa which is very close to the predicted value, hence the model is validated.

Table 6 : Optimum tensile strength of the friction welded SUS 304HCu tube

	Rottional speed 'R' (RPM)	Friction pressure (MPa)	Forging pressure (MPa)	Friction time 'F' (s)	Forging time 'D' (s)
Predicted by RSM	2112	32	47	23.73	55.1
Experimental	2110	32	47	24	55

Table 7 : Tensile properties of the friction welded SUS 304HCu tube welded using optimized parameters

Tensile test at room temperature	0.2% Yield strength (MPa)	Tensile strength (MPa)	% Elongation in gauge length of 30 mm
Result	286	599	25

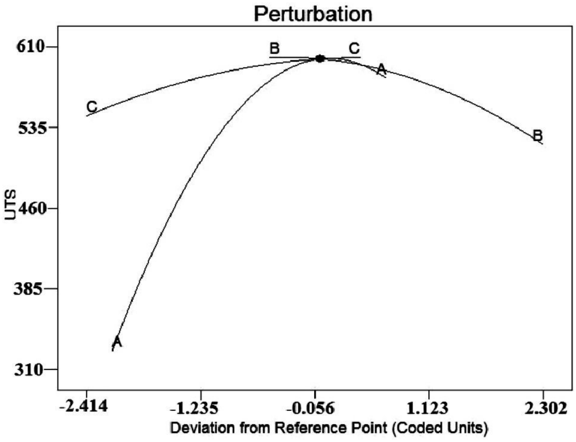

Fig.4 : Perturbation plot showing the effect of all factors on the tensile strength

5.0 CONCLUSIONS

1. The SUS 304HCu austenitic stainless steel tubes having 57.1 mm outer diameter and 3.5 mm thick was successfully welded using friction welding process.
2. An empirical relationship incorporating the friction welding parameters was developed to predict the tensile strength of friction welded SUS 304HCu austenitic stainless steel tubes at 95% confidence level.
3. It was found that the rotational speed was the most influencing factor to affect the tensile strength of the joint based on the calculated F value (18340).
4. The developed model predicted the optimum friction welding parameters for achieving maximum tensile strength in friction welded SUS 304HCu tubes as R = 2112 RPM, F = 23.73 s, and D = 55.1 s with friction and forging pressure of 32 MPa and 47 MPa respectively.
5. The friction welded SUS 304HCu joint fabricated using optimized parameters exhibited a joint efficiency of 98% (599 MPa).

ACKNOWLEDGEMENTS

The authors wish to express their sincere thanks to M/s Mailam India Ltd, Pondicherry, India for providing fund to carry out this research work through Mailam India Research (MIR) fellowship and M/s Salzgitter Mannesmann Stainless Tubes Italia Srl of Italy for supplying the SUS 304HCu tubes required to carry out this work.

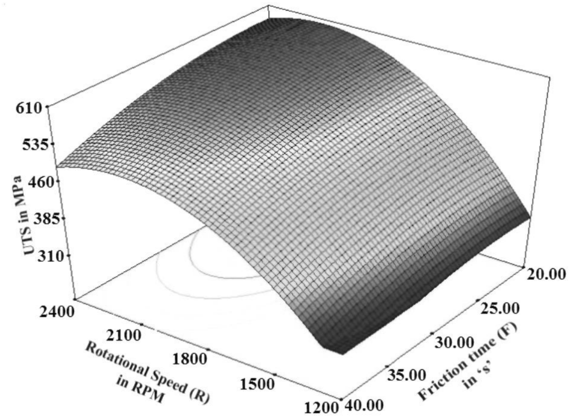

a. Response plot showing the effect of R and F on tensile strength at D = 55.1 s

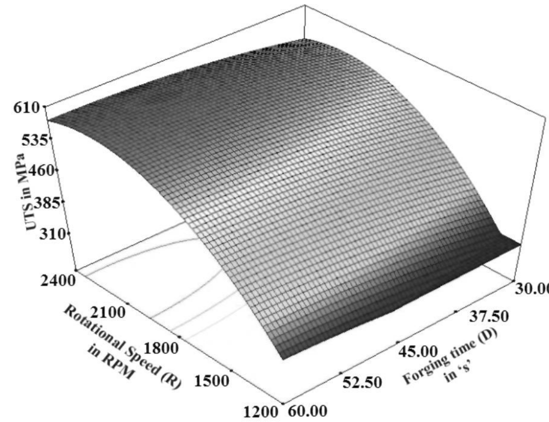

b. Response plot showing the effect of R and D on tensile strength at F = 23.73 s

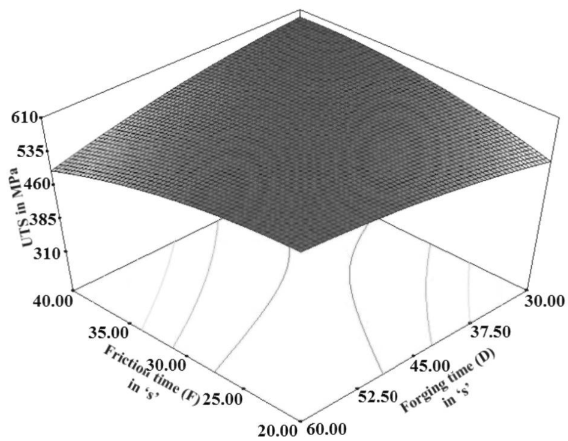

c. Response plot showing the effect of F and D on tensile strength at R = 2112.23 RPM

Fig. 5 : Response plots for the regression generated using statistical software

REFERENCES

1. Viswanathan R, and Bakker W. (2001); Materials for ultrasupercritical coal power plants boiler materials part 1, J Mater Eng Perform, 10, pp.81-95.
2. Koen Faes, Alfred Dhooge, Patrick De Baets and Paul Afschrift. (2009); New friction welding process for pipeline girth welds-welding time optimisation, J Adv Manuf Technol, 43, pp.982-92.
3. Kimura M, Ichihara A, Kusaka M and Kaizu K. (2012); Joint properties and their improvement of AISI 310S austenitic stainless steel thin walled circular pipe friction welded joint, J Mater Design, 38, pp.38-46.
4. Yuanzhi zhu, Yingying guo and Libin yang. (2013); Microstructure based strength distribution across the welds of Nickel-Based Superalloy Inconel 751 and austenite Steel 21-4N Joined by Inertia friction Welding, J Metall Mater Trans B, 44, pp.396-405.
5. Mumin Sahin. (2007); Evaluation of the joint interface properties of austenitic-stainless steels (AISI 304) joined by friction welding, J Mater Design, 28, pp.2244–2250.
6. Satyanarayana, V. V., Madhusudhan Reddy G, and Mohandas T. (2005); Dissimilar metal friction welding of austenitic ferritic stainless steels, J Mater Process Technol, 160, pp.128-137.
7. Paulraj Sathiya, Aravindan S, and Noorul Haq A. (2006); Optimization for friction welding parameters with multiple performance characteristics, Int J Mech Mater Des, 3, pp.309-318.
8. Padmanaban G, and Balasubramanian V. (2011); Optimization of pulsed current gas tungsten arc welding process parameters to attain maximum tensile strength in AZ31B magnesium alloy, Trans Nonferrous Met Soc China, 21, pp.467–476.
9. Sathiya P, Aravindan S, and Noorul Haq A. (2007); Effect of friction welding parameters on mechanical and metallurgical properties of ferritic stainless steel, Int J Adv Manuf Technol, 31, pp.1076–1082.
10. Montgomery, D. C. (2001); Design and analysis of experiments, 4th ed, New York, Jhon wiley & sons.
11. Benyounis, K.Y., Olabi, A.G., and Hashmi, M.S.J. (2008); Multi response optimization of CO2 Laser-welding process of austenitic stainless steel, J Opt laser technol, 40, pp.76-87.
12. Padmanaban G. and Balasubramanian V. (2010); Prediction of tensile strength and optimization of process parameters for friction stir welded AZ31B magnesium alloy, Proc Inst Mech Eng B J Eng Manuf, 224, pp.1519-1528.
13. Lakshminarayanan, A. K. and Balasubramanian V. (2009); Comparison of RSM with ANN in predicting tensile strength of friction stir welded AA7039 aluminium alloy joints, Trans Nonferrous Met Soc China, 19, pp.9-18.
14. Elangovan K., Balasubramanian V. and Babu S. (2009); Predicting tensile strength of friction stir welded AA6061 aluminium alloy joints by a mathematical model, J Mater Design, 30, pp.188-193.
15. Paventhan R., Lakshminarayanan, P. R. and Balasubramanian V. (2011); Prediction and optimization of friction welding parameters for joining aluminium alloy and stainless steel, J Trans. Nonferrous Met. Soc. China, 21, pp.1480–1485.